JACS
JOURNAL OF THE AMERICAN CHEMICAL SOCIETY
Communication
pubs.acs.org/JACS

Delayed Onset of Crystallinity in Ion-Containing Aqueous Nanodrops

Richard J. Cooper, Matthew J. DiTucci, Terrence M. Chang, and Evan R. Williams*

Department of Chemistry, University of California, Berkeley, California 94720-1460, United States

Supporting Information

ABSTRACT: Water exhibits remarkable properties in confined spaces, such as nanometer-sized droplets where hundreds of water molecules are required for crystalline structure to form at low temperature due to surface effects. Here, we investigate how a single ion affects the crystallization of $(H_2O)_n$ clusters with infrared photodissociation spectroscopy of size-selected $La^{3+}(H_2O)_n$ nanodrops containing up to 550 water molecules. Crystallization in the ion-containing nanodrops occurs at $n \geq 375$, which is approximately 100 more water molecules than what has been reported for neutral water clusters. This frustration of crystallinity reveals that La^{3+} disrupts the hydrogen-bonding network of water molecules located remotely from the ion, a conclusion that is supported by molecular dynamics simulations. Our findings establish that a trivalent ion can pattern the H-bond network of water molecules beyond the third solvation shell, or to a distance of ~1 nm from the ion.

Water clusters containing charged particles are involved in numerous phenomena central to atmospheric and space sciences. Ion-induced nucleation is a major pathway to the formation of aerosol particles because electrostatic forces can stabilize embryonic particles with diameters between 1 and 2 nm and accelerate their growth rates.[1] Upon further growth, such particles drive diverse processes ranging from ion-enhanced chemical reactions on sea spray droplets[2] to the production of ozone-depleting chlorine species on the surfaces of ice nanoparticles.[3] When confined to nanometer-sized spaces, the properties of water differ significantly from those in bulk solution owing to the large interfacial area that disrupts optimal hydrogen-bonding.[4] In small water clusters cooled well below the solvent's bulk freezing point, the formation of crystalline ice is inhibited by the tendency for dangling O−H bonds at the surface to optimize H-bonding interactions.[5] The minimum number of water molecules needed to support crystallization within a neutral water cluster has been the subject of experimental and theoretical studies. Electron diffraction experiments[6] on water clusters formed in a free jet expansion indicate that the onset of crystallization occurs between n = 200 and 1000, and FT-IR spectra of ice nanoparticles along with calculations by Buch et al. are in agreement with this size range.[5a,b] A complicating factor in interpreting these experiments is that the cluster size must be estimated. This obstacle was recently surmounted by Pradzynski et al., who measured infrared spectra of neutral water clusters doped with sodium atoms.[7] The clusters were separated and mass analyzed after infrared-modulated photoionization. They reported that the onset of crystallization occurs at $n = 275 \pm 25$ and that the clusters are predominately crystalline by n = 475, the largest size investigated. The temperature of the water clusters in this experiment was estimated to be 90−115 K, and the onset of crystallization may occur at smaller cluster sizes for higher temperatures.[8]

Ions are well known to reduce the freezing point of water, but the extent to which ion-induced patterning of the water molecule network disrupts crystallization within a cold nanodrop has not been previously investigated. Infrared photodissociation (IRPD) spectroscopy is a sensitive structural probe of hydrated gaseous ions, and IR spectroscopies of hydrated ions have yielded detailed structural information about how H-bond networks are arranged around ions.[9] IRPD results indicate that both the charge state[10] and size[10a] of an ion affect its hydration and that the H-bonding network of water molecules is minimally perturbed by some ions,[9d] but can be affected past the first solvation shell by others.[9e,f] Thus, one might expect that in aqueous nanodrops, where an ion is internally solvated, the crystallization of water will be hindered and that this effect will be more pronounced for high valency ions. The extent to which an ion can disrupt the H-bonding network of water molecules located remotely from the ion has implications for a wide variety of phenomena, most notably Hoffmeister series effects of ions on protein solubilities.[11] Our laboratory has developed an experimental technique (see Supporting Information, SI) for studying extensively hydrated ions[9e,f,10b] in isolation at a well-defined temperature without the complicating presence of counterions. Herein, we use IRPD spectroscopy to characterize how La^{3+} perturbs the H-bonding network in $(H_2O)_n$ clusters with n = 50−550. La^{3+} was chosen because of its high valency and single dominant isotope, which results in improved signal-to-noise ratios for these measurements.

The electrospray-generated $La^{3+}(H_2O)_n$ clusters are trapped in the ion cell of a 7.0 T Fourier transform ion cyclotron resonance mass spectrometer, where they are thermalized at 133 K, size-selected, and photodissociated with a tunable infrared laser (SI). The IRPD spectra of $La^{3+}(H_2O)_n$ (Figure 1) can be divided into two distinct regions. The relatively sharp resonances in the spectra between ~3650 and 3750 cm^{-1} arise from dangling "free" O−H oscillators on the surface of the nanodrop that are not H-bonded. The much broader bands between ~3000 and 3650 cm^{-1} are due to H-bonded O−H oscillators throughout the nanodrop. The ratio of the intensities of the free O−H to bonded O−H bands decreases with increasing cluster size because the fraction of water molecules

Received: November 12, 2015
Published: December 29, 2015

DOI: 10.1021/jacs.5b11880
J. Am. Chem. Soc. 2016, 138, 96−99

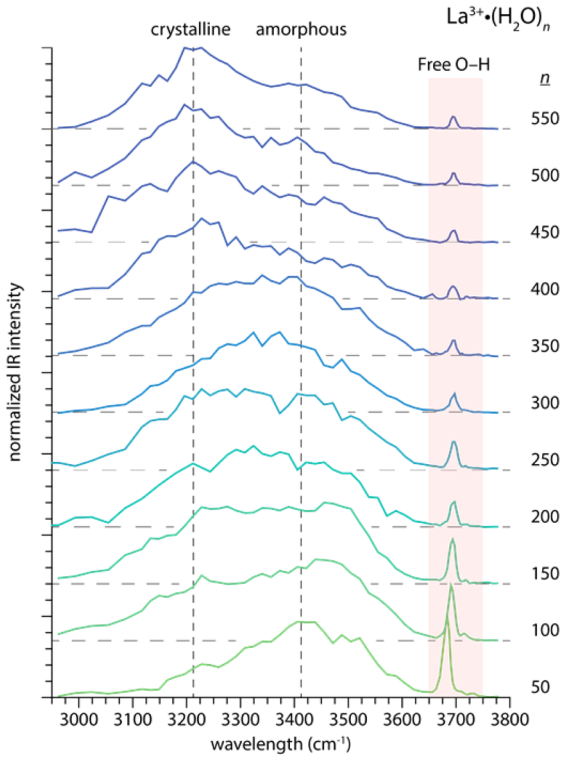

Figure 1. IRPD spectra of $La^{3+}(H_2O)_n$ for $50 \leq n \leq 550$ measured at 133 K. The sharp bands between 3650 and 3750 cm^{-1} correspond to free O−H stretches of water molecules located exclusively on the surface of the nanodrops, whereas the broader resonances between 3000 and 3650 cm^{-1} arise from H-bonded O−H stretches throughout the clusters. Crystalline and amorphous ice bands are marked with vertical dashed lines.

on the surface of the nanodrops decreases relative to those in the interior. There is also a shift in the frequency of the free O−H band. In the spectrum of $La^{3+}(H_2O)_{50}$, this band is centered on 3683 cm^{-1}, and blue-shifts with increasing cluster size up to n = 250, where it has a value of 3696 cm^{-1}, close to that obtained from SFG measurements at the air−water interface.[12] The frequency shift of the free O−H band is attributable to a Stark shift from the ion's electric field, which is more pronounced for smaller cluster sizes.[10]

Changes in the bonded O−H region with cluster size reflect size-dependent structural changes that occur in the H-bonding networks. The IRPD spectrum of $La^{3+}(H_2O)_{50}$ has a broad band centered on ~3410 cm^{-1} that is consistent with similar bands in infrared and Raman spectra of amorphous ice and liquid water that have a maximum near 3400 cm^{-1}.[13] Crystalline ice has an absorption maximum near 3200 cm^{-1},[13] a region with little intensity in the spectrum of $La^{3+}(H_2O)_{50}$. This suggests that water molecules in this cluster adopt a phase that is close to that of liquid water or amorphous ice. The intensity between 3000 and 3400 cm^{-1} increases with cluster size, and for $200 \leq n \leq 350$, the spectra contain one very broad (~400 cm^{-1}) symmetric band with a maximum near 3350 cm^{-1}. Studies of neutral ice nanoparticles indicate that strained subsurface crystalline ice has a spectroscopic signature similar to crystalline ice,[5a,b] and the emergence of strained ice-like water may contribute to the increased intensity between 3000 and 3400 cm^{-1} with increasing cluster size. At n = 400, there is a significant spectral change where a distinct band centered on 3220 cm^{-1} appears that is the most intense feature in the spectrum. This band, which is attributed to crystalline ice,[7] continues to grow in intensity relative to the amorphous ice band up through the largest cluster size measured at n = 550. The emergence of a distinct crystalline ice band at 3200 cm^{-1} was used to identify the onset of crystallinity in neutral droplets.[7] Accordingly, we conclude that the onset of crystallinity occurs at $n \approx 375$ in these ion-doped aqueous nanodrops, 100 water molecules greater than the onset of crystallinity reported for neutral water clusters at a comparable temperature.[7]

The spectral red-shift of ~200 cm^{-1} accompanying the onset of crystallinity in these $La^{3+}(H_2O)_n$ clusters is remarkably similar to that measured in temperature-dependent infrared and Raman spectra of bulk water,[13] and temperature-dependent SFG spectra at the air/water interface.[14] A similar red-shift also occurs in FT-IR spectra of ice nanoparticles as the size distribution increases from tens to thousands of water molecules.[5a] The delayed onset of crystallinity in the lanthanum-containing nanodrops relative to neutral nanodrops can be rationalized as a result of the perturbation induced by the internally solvated ion that disrupts the formation of crystalline ice in the interior of the nanodrop. The extent to which ions affect the H-bonding network of water molecules located remotely from the ion is hotly debated with reports based on femtosecond infrared,[15] terahertz absorption,[16] and Raman[17] measurements concluding that the structuring effect is limited to the first solvation shell. Our present results show that a single La^{3+} ion exerts a long-range influence on water molecules that extends well beyond the first solvation shell, consistent with IRPD studies of hydrated polyatomic anions and anionic complexes,[9e,f] dielectric relaxation spectroscopy of aqueous salt solutions,[18] and X-ray scattering measurements of long-range solvent ordering around colloidal nanoparticles.[19] The extent of ion-induced patterning of water will decrease with increasing temperature,[9f] and this may explain some of the discrepancies between conclusions drawn from our experiments and those performed near room temperature.

For a spherical nanodrop, the ratio of the area of the free O−H band (3650−3750 cm^{-1}) to the area of the bonded O−H band (3000−3650 cm^{-1}) should decrease linearly with $1/r$ provided that the fraction of surface water molecules with a free O−H bond remains constant. These data as a function of $n^{-1/3}$ ($\propto 1/r$) for $La^{3+}(H_2O)_n$ clusters are shown in Figure 2. This ratio of spectral intensities is linear for $n \geq 100$ indicating that these nanodrops are approximately spherical, consistent with transmission electron microscopy images of larger ice nanoparticles ($r \approx$ 15−30 nm).[20] The exception to the linear trend is $La^{3+}(H_2O)_{50}$ for which the area under the free O−H band is anomalously large. The higher intensity of the free O−H band for this ion is attributed to the strong influence of the ion's electric field on the surface of the cluster that orients additional O−H bonds outward.[10] The effect of the ion on the orientations of surface water molecules may also affect their spectral intensities.

In order to estimate the distance to which La^{3+} patterns the H-bonding network of water molecules located remotely from the ion, molecular dynamics simulations were performed on $Mo^{3+}(H_2O)_{550}$ at 133 K. Mo^{3+} is the largest trivalent ion parametrized in the OPLS 2005 force field and is slightly smaller than La^{3+} (SI). From a 60 ns trajectory, 1000 structures were generated and the effect of the ion on the orientations of water molecules located at a distance d from the ion was evaluated by calculating the angle θ between the dipole vector

DOI: 10.1021/jacs.5b11880
J. Am. Chem. Soc. 2016, 138, 96−99

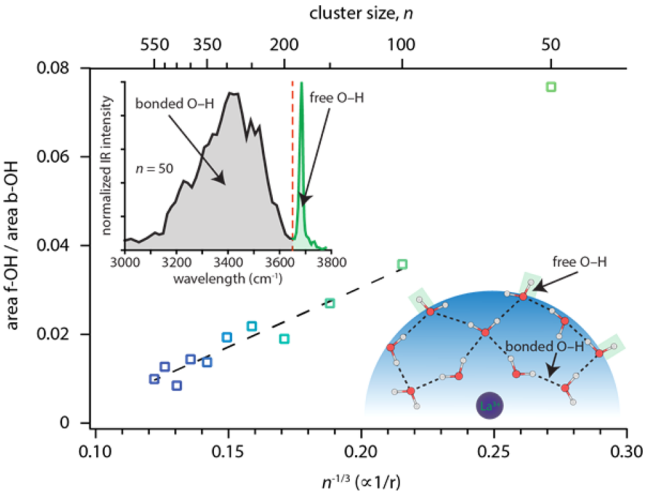

Figure 2. Ratio of integrated band intensities of the free O–H stretches (3650–3750 cm^{-1}) to bonded O–H stretches (3600–3650 cm^{-1}) in each $La^{3+}(H_2O)_n$ IRPD spectrum as a function of $n^{-1/3}$, which is proportional to $1/r$. The two spectral bands that are integrated are shown in the top left inset, and the bottom right inset depicts the different types of O–H stretches that give rise to these bands. The average cluster size, n, is indicated in the top abscissa. A linear least-squares fit ($R^2 = 0.93$) for clusters with n between 100 and 550 is shown by the dashed line.

of each water molecule and the vector defined by the metal–oxygen displacement (Figure 3, inset) for every structure. A histogram of $\langle\theta\rangle$ values as a function of distance from the metal ion for the 1000 structures is shown in Figure 3.

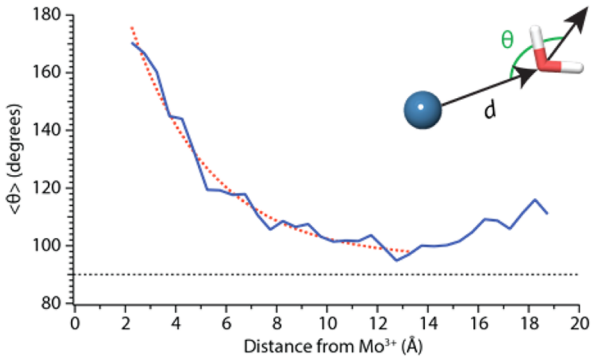

Figure 3. Average angle θ (shown in inset) calculated from 1000 structures of $Mo^{3+}(H_2O)_{550}$ as a function of distance from the metal ion in bin sizes of 0.5 Å. The dotted red line is an exponential fit to these data between 2.25 and 13.5 Å, and the horizontal dotted black line marks $\langle\theta\rangle = 90°$.

Water molecules in the inner hydration shell are strongly oriented "outward" by the ion, with $\langle\theta\rangle$ near 170°. This orientation bias decays exponentially with increasing distance from the ion up until ~14 Å, where the angles becomes larger again near the surface of the nanodrop. At the surface, under-coordinated "dangling" water molecules are oriented with their O–H bonds pointing away from the ion. *Ab initio* dynamics simulations would result in a more accurate description of H-bonding interactions in these clusters, and may predict the onset of a crystalline phase, but are prohibitively expensive for clusters of this size. The initial decrease to ~14 Å is attributed to ion-induced patterning of the H-bond network in the nanodrop that decreases with distance from the ion. To characterize the spatial extent of ion-induced patterning in these nanodrops, the data for d < 13.5 Å were fit with an exponential function, thereby excluding surface effects. The decay constant τ from the fit is 3.19 Å. When adjusted for the 2.25 Å offset between the first shell water molecules and the ion, the τ value indicates that the orientation bias of water molecules drops to ~37% of its maximal value at a distance of 5.4 Å from the ion. This distance corresponds to the third hydration shell, as shown in the calculated radial distribution function for a representative structure of $Mo^{3+}(H_2O)_{550}$ (Figure 4).

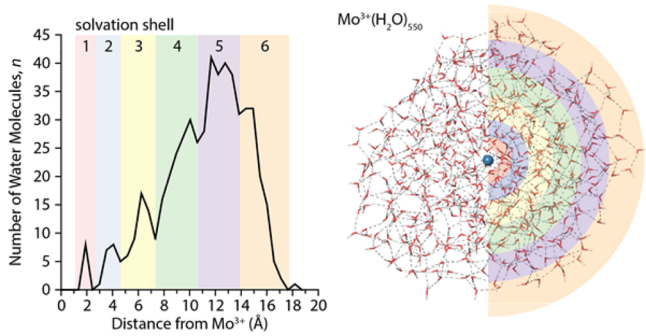

Figure 4. Radial distribution function of Mo^{3+}–O distances binned in 0.5 Å increments (left) for a representative structure of $Mo^{3+}(H_2O)_{550}$ (right). Minima in the distribution function indicate transitions between solvation shells, which are numbered and color-coded.

The results from this dynamics simulation predict that trivalent metal ions can pattern the H-bonding network strongly out to *at least* the third hydration shell which, for Mo^{3+}, includes ~60 water molecules. The strength of this patterning effect diminishes exponentially with distance from the ion, and competition between ion-water patterning and crystallization may result in less extensive patterning than our calculations suggest. These calculations are consistent with the delayed onset of crystallinity in the $La^{3+}(H_2O)_n$ clusters deduced from the IRPD data.

Our combined experimental and theoretical results indicate that La^{3+} exerts a strong influence on the H-bonding network of water molecules located remotely from the ion, thereby frustrating crystallization in aqueous nanodrops. The extent of solvent patterning will depend on the ion charge state and to a lesser extent ion size.[10] There is some experimental evidence indicating that divalent ions can affect the structure of water outside the first solvation shell.[9e,10,18] Future investigations should provide new insights into how the crystallization process in confined nanoscale systems depends on temperature as well as ion charge state and size.

■ ASSOCIATED CONTENT

Supporting Information

The Supporting Information is available free of charge on the ACS Publications website at DOI: 10.1021/jacs.5b11880.

Procedures for IRPD spectroscopy and MD simulations and xyz coordinates for the structure in Figure 4 (PDF)

■ AUTHOR INFORMATION

Corresponding Author

*erw@berkeley.edu

DOI: 10.1021/jacs.5b11880
J. Am. Chem. Soc. 2016, 138, 96–99

Notes

The authors declare no competing financial interest.

■ ACKNOWLEDGMENTS

The authors thank the National Science Foundation (grant CHE-1306720) for generous financial support of this research. We express our gratitude to Dr. Jeremy T. O'Brien and Richard A. O'Brien for the design of a preamplifier.

■ REFERENCES

(1) (a) Lee, S. H.; Reeves, J. M.; Wilson, J. C.; Hunton, D. E.; Viggiano, A. A.; Miller, T. M.; Ballenthin, J. O.; Lait, L. R. *Science* **2003**, *301*, 1886. (b) Yu, F. Q.; Turco, R. P. *J. Geophys. Res.* **2001**, *106*, 4797.
(2) Knipping, E. M.; Lakin, M. J.; Foster, K. L.; Jungwirth, P.; Tobias, D. J.; Gerber, R. J.; Dabdub, D.; Finlayson-Pitts, B. J. *Science* **2000**, *288*, 301.
(3) Gertner, B. J.; Hynes, J. T. *Science* **1996**, *271*, 1563.
(4) (a) Algara-Siller, G.; Lehtinen, O.; Wang, F. C.; Nair, R. R.; Kaiser, U.; Wu, H. A.; Geim, A. K.; Grigorieva, I. V. *Nature* **2015**, *519*, 443. (b) Levinger, N. E. *Science* **2002**, *298*, 1722.
(5) (a) Buch, V.; Sigurd, B.; Paul Devlin, J.; Buck, U.; Kazimirski, J. K. *Int. Rev. Phys. Chem.* **2004**, *23*, 375. (b) Devlin, J. P.; Joyce, C.; Buch, V. *J. Phys. Chem. A* **2000**, *104*, 1974. (c) Buch, V.; Delzeit, L.; Blackledge, C.; Devlin, J. P. *J. Phys. Chem.* **1996**, *100*, 3732.
(6) (a) Torchet, G.; Schwartz, P.; Farges, J.; Deferaudy, M. F.; Raoult, B. *J. Chem. Phys.* **1983**, *79*, 6196. (b) Torchet, G.; Farges, J.; Deferaudy, M. F.; Raoult, B. *Ann. Phys.* **1989**, *14*, 245.
(7) Pradzynski, C. C.; Forck, R. M.; Zeuch, T.; Slavicek, P.; Buck, U. *Science* **2012**, *337*, 1529.
(8) Buck, U.; Pradzynski, C. C.; Zeuch, T.; Dieterich, J. M.; Hartke, B. *Phys. Chem. Chem. Phys.* **2014**, *16*, 6859.
(9) (a) Fournier, J. A.; Johnson, C. J.; Wolke, C. T.; Weddle, G. H.; Wolk, A. B.; Johnson, M. A. *Science* **2014**, *344*, 1009. (b) Tielrooij, K. J.; Garcia-Araez, N.; Bonn, M.; Bakker, H. J. *Science* **2010**, *328*, 1006. (c) Shishido, R.; Li, Y. C.; Tsai, C. W.; Bing, F.; Fujii, A.; Kuo, J. L. *Phys. Chem. Chem. Phys.* **2015**, *17*, 25863. (d) Prell, J. S.; Williams, E. R. *J. Am. Chem. Soc.* **2009**, *131*, 4110. (e) O'Brien, J. T.; Prell, J. S.; Bush, M. F.; Williams, E. R. *J. Am. Chem. Soc.* **2010**, *132*, 8248. (f) DiTucci, M. J.; Heiles, S.; Williams, E. R. *J. Am. Chem. Soc.* **2015**, *137*, 1650.
(10) (a) Prell, J. S.; O'Brien, J. T.; Williams, E. R. *J. Am. Chem. Soc.* **2011**, *133*, 4810. (b) O'Brien, J. T.; Williams, E. R. *J. Am. Chem. Soc.* **2012**, *134*, 10228.
(11) Marcus, Y. *Chem. Rev.* **2009**, *109*, 1346.
(12) Ji, N.; Ostroverkhov, V.; Tian, C. S.; Shen, Y. R. *Phys. Rev. Lett.* **2008**, *100*, 096102.
(13) (a) Brubach, J. B.; Mermet, A.; Filabozzi, A.; Gerschel, A.; Roy, P. *J. Chem. Phys.* **2005**, *122*, 184509. (b) D'Arrigo, G.; Maisano, G.; Mallamace, F.; Migliardo, P.; Wanderlingh, F. *J. Chem. Phys.* **1981**, *75*, 4264.
(14) Wei, X.; Miranda, P. B.; Zhang, C.; Shen, Y. R. *Phys. Rev. B: Condens. Matter Mater. Phys.* **2002**, *66*, 085401.
(15) Omta, A. W.; Kropman, M. F.; Woutersen, S.; Bakker, H. J. *Science* **2003**, *301*, 347.
(16) (a) Funkner, S.; Niehues, G.; Schmidt, D. A.; Heyden, M.; Schwaab, G.; Callahan, K. M.; Tobias, D. J.; Havenith, M. *J. Am. Chem. Soc.* **2012**, *134*, 1030. (b) Sharma, V.; Bohm, F.; Seitz, M.; Schwaab, G.; Havenith, M. *Phys. Chem. Chem. Phys.* **2013**, *15*, 8383.
(17) Smith, J. D.; Saykally, R. J.; Geissler, P. L. *J. Am. Chem. Soc.* **2007**, *129*, 13847.
(18) Buchner, R. *Pure Appl. Chem.* **2008**, *80*, 1239.
(19) Zobel, M.; Neder, R. B.; Kimber, S. A. *Science* **2015**, *347*, 292.
(20) Delzeit, L.; Blake, D. *J. Geophys. Res.* **2001**, *106*, 33371.

DOI: 10.1021/jacs.5b11880
J. Am. Chem. Soc. 2016, 138, 96−99